

Mechanical properties of porous titanium with different distributions of pore size

Xiao-hua WANG, Jin-shan LI, Rui HU, Hong-chao KOU, Lian ZHOU

State Key Laboratory of Solidification Processing, Northwestern Polytechnical University, Xi'an 710072, China

Received 13 June 2012; accepted 3 September 2012

Abstract: To satisfy the mechanical and biological requirement of porous bone substitutes, porous Ti with two different pore sizes designed in advance was fabricated by the space-holder sintering process. Mechanical properties of the porous Ti were explored via room temperature compressive tests. The pore sizes and shapes are uniform throughout the specimens with porosities ranging from 36% to 63%. The compression strength and the elastic modulus are in the range from 94.05 to 468.57 MPa and 2.662 to 18 GPa, respectively. It is worth noting that the relationship between the compressive strength and the porosities is completely linear relation beyond the effect of pore size distributions on the mechanical properties. The value of the constant C achieved from the Gibson-Ashby model suggests that the pore sizes affect the yield strength of the porous Ti and the values of density exponent (n) for porous Ti with two different pore sizes are higher than 2, which suggests that the deformation mode of the porous Ti with a porosity ranging from 36% to 63% is mainly buckling of the cell struts.

Key words: porous Ti; pore size distributions; mechanical properties; density exponent; biomaterials

1 Introduction

Titanium and its alloys are widely used as orthopedic and dental implant materials due to their excellent mechanical properties, biocompatibility and good corrosion resistance. However, the mismatch of mechanical properties between the bone tissue and implant materials results in tissue loss (a low interface adhesive strength and a loose surface) due to the stress shield [1]. One effective measurement to avoid the stress shield is to develop porous implants [2–4]. The mechanical properties of porous implants are possible to adjust by selecting the porosity. The interconnected pores permit bone ingrowth into the pores and provide not only anchorage for the fixation but also a system which enhances stress redistributions to the adjacent bone tissues, therefore minimizes stress shielding and eventually prolongs device lifetime. In addition, the interconnected pore structure allows the transport of body fluids within the pore structure.

In order to guarantee biocompatibility, the porous implants should mimic bone morphology, structure and function to optimize integration into surrounding tissue.

Porosity and pore size both in the macroscopic and the microscopic level, are important morphological properties for implant materials to bone regeneration. Large pores (100–600 μm) show substantial bone ingrowth, while smaller pores result in ingrowth of unmineralized osteoid tissue (75–100 μm) and fibrous tissue (10–75 μm) [5]. The minimum pore size required to regenerate mineralized bone is generally considered to be 100 μm according to the study of ITÄLÄ et al [6]. Meanwhile, pore morphology, pore size and porosity are properties-determined factors. To date, researchers have studied the mechanical properties of porous titanium with different porosities and/or different pore sizes [2,6–11]. But the effect of the different distributions of pore size on mechanical properties of porous titanium has not been clear. So, in this work, two distributions of pore size which is beneficial to the bone ingrowth were selected, and the porous titanium with different pore sizes is developed by powder sintering method, which is controlled by the distributions of space-holder size. The aim of this study is to investigate mechanical properties of porous titanium implant with different distributions of pore size and the deformation mode of the cell wall of the porous titanium implant.

2 Experimental

2.1 Specimen preparation

Porous titanium samples with porosities of 36%–63% were manufactured by the powder metallurgy and the space holder technique. Commercially available pure titanium (purity $\geq 99.9\%$, powder size $\leq 45 \mu\text{m}$) was used as raw material and soluble sodium chloride particles with different sizes and contents were used as spacer materials. To attain the different pore size distributions of porous titanium, the sodium chloride powder was sieved to select similar particle sizes in the range of 100–200 μm and 350–450 μm . Ti powders and spacer particles were thoroughly mixed in an agate mortar. After the ingredients were homogeneously blended, powders of the mixture were uniaxially pressed at a pressure of 180 MPa into green compacts. Then the green compacts were sintered into porous Ti. The sintering process consisted of two steps, i.e., at 1073 K for 8 h and 1473 K for 8 h. There was an important step between the two steps of sintering, which was desalting in the distilled water. In addition, the sinter process was in a vacuum of 10^{-3} Pa.

2.2 Mechanical testing

Mechanical properties of porous Ti were studied by the compression test. Compression tests were performed on six samples from each of the three sample groups with different pore size distributions: 100–200 μm and 350–450 μm at room temperature. Tests specimens had sizes of $d13 \text{ mm} \times 13 \text{ mm}$ (GB 6526–86). The initial strain rate for compression tests was of 10^{-3} s^{-1} . Compressive strength refers to the local stress maximum after the linear elastic region of the curve. Elastic modulus was calculated as the slope of the linear elastic region [3]. Porosity was evaluated according to the apparent densities method prescribed in previous study [2]. The morphology and pore size of the porous Ti were observed by scanning electron microscopy (SEM).

2.3 Analytical modeling

As predicted by GIBSON and ASHBY [12], the relationship between the relative properties and the relative density (ρ/ρ_s) for open-cell foam was

$$\sigma_{\text{pl}}/\sigma_{\text{ys}} = C(\rho/\rho_s)^n \quad (1)$$

where σ_{pl} is the plateau stress of the porous material; σ_{ys} is the yield strength of the cell surface solid material; and C and n are constants depending on the cell structure. To date, the complex dependence of C and n on structures has not been well understood. Experimental evidence suggests that n is 1.5 for open-cell foams, and C is a constant of 0.3 for cellular metals and polymers.

3 Results and discussion

3.1 Microstructure

Figure 1 shows the typical SEM images of the porous titanium with the porosity range of 36%–63% for the two different pore size distributions designed in advance, Figs. 1(a)–(d) for 100–200 μm and Figs. 1(e)–(h) for 350–450 μm . In order to distinguish the two different pore size distributions, the pore size distributions in this work are marked 100–200 μm and 350–450 μm which are designed in advance. Statistical analysis of pore sizes reveals that the porous Ti sintered using space-holder particles of 100–200 μm and 350–450 μm gives pore sizes of 155 μm and 400 μm , respectively. The pore sizes are a little smaller than those of spacer particles, probably owing to specimen shrinkage during sintering. The pore structures were evenly distributed throughout the specimen with porosities ranging from 36% to 63%. The morphologies of pores located on the surface and within the porous scaffolds exhibit good pore interconnectivity as shown in SEM images.

Pore size of biomaterials plays a critical role in bone formation in vitro and in vivo [5]. There are two types of pore in the porous Ti which are large pores and small pores. Large pores with size of 100–600 μm lead to direct osteogenesis, while small pores less than 100 μm favor hypoxic conditions and induce osteochondral formation before osteogenesis. It could be hypothesized that the porous titanium with similar three-dimensional and connective network configuration may avail osteogenesis and it would be expected to provide paths for efficient bone ingrowth [8].

3.2 Mechanical properties

Figure 2 shows the compressive stress—strain curves of porous Ti with different porosities and two different pore size distributions designed in advance. The curves show the typical features of metallic foams [7], which start with linear elastic deformation, and follow plateau stage with a smooth flow stress as the strain increases. In this region the pores are compressed and distorted, and then a densification stage. For porous materials, the plateau region is the typical characteristics. From Fig. 2, it can be found that the extension happens in the plateau region and becomes more evident with the increase of porosity. In this work, plateau region is defined as the region from the peak stress to the following second peak stress. The strains of the plateau region are 8%, 10%, 10.22% and 30.5% for porosities of 39%, 45%, 55% and 63%, respectively. In a similar way, the strains of the plateau region for pore sizes of 10–200 μm are 9%, 10%, 11.3% and 32.5% for porosities of

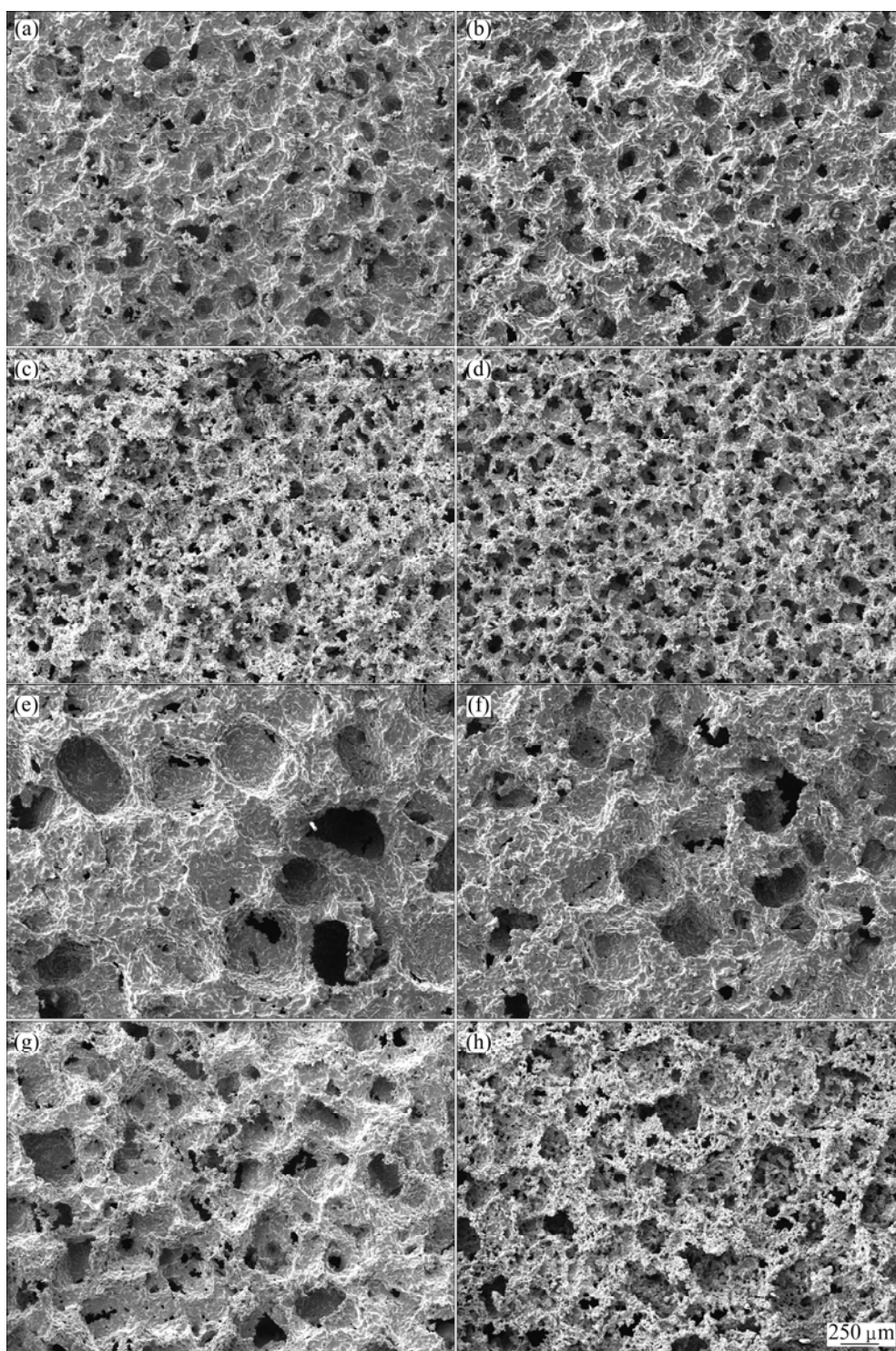


Fig. 1 Pore structure of porous Ti samples with different pore size distributions and porosities: (a–d) 100–200 μm ; (e–h) 350–450 μm ; (a) 36%; (b) 41%; (c) 50%; (d) 60%; (e) 39%; (f) 45%; (g) 55%; (h) 63%

36%, 41%, 50% and 63%, respectively.

3.2.1 Elastic modulus

Figure 3 shows the elastic modulus of the porous Ti with different porosities. In this work, the slope of the linear elastic region of curves was taken as a measurement of the elastic moduli of porous Ti. The measured elastic moduli are found to be 2.762–16.77

GPa and 2.662–18 GPa for the porous Ti samples having pore sizes ranging from 100 to 200 μm and 350 to 450 μm , respectively. The elastic modulus increased with the decrease in porosity. The specimens with a low porosity of 36% showed the high elastic modulus of 16.77 GPa. When the porosity increased from 36% to 60%, the elastic modulus was only 2.762 GPa. Specimens with

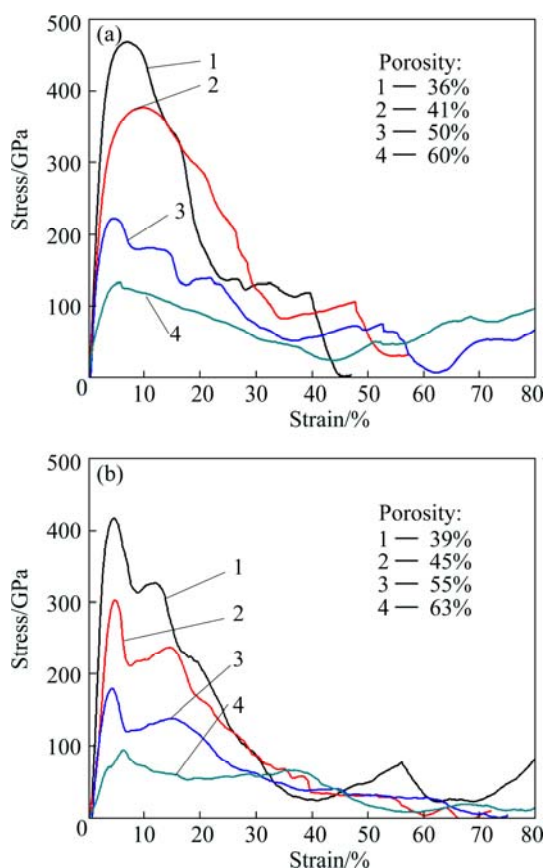


Fig. 2 Compressive strain–stress curves of porous Ti with pore size distributions of 100–200 μm (a) and 350–450 μm (b)

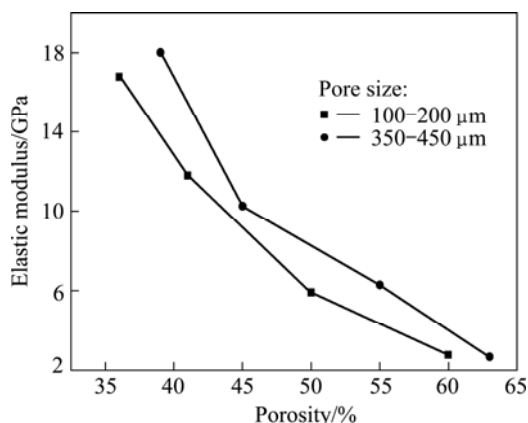


Fig. 3 Elastic modulus of sintered porous titanium as function of porosity

different pore sizes from 350 to 450 μm had the same trend. In comparison with the smaller pore size distributions, the elastic modulus of porous Ti showed a higher value, when its pore size was in the range of 350–450 μm.

3.2.2 Compressive strength

Figure 4 shows the compressive strength of the porous titanium with different porosities. The compression strength is in the range from 132.95 to 468.57 MPa and 94.05 to 416.57 MPa for the porous Ti

with the pore sizes in the range of 100–200 μm and 350–450 μm, respectively. The compression strength decreases linearly with increasing porosity. However, unlike the relationship between the elastic modulus and porosities, the relationship between the compressive strength and porosities is completely linear relation beyond the effect of the pore size distributions.

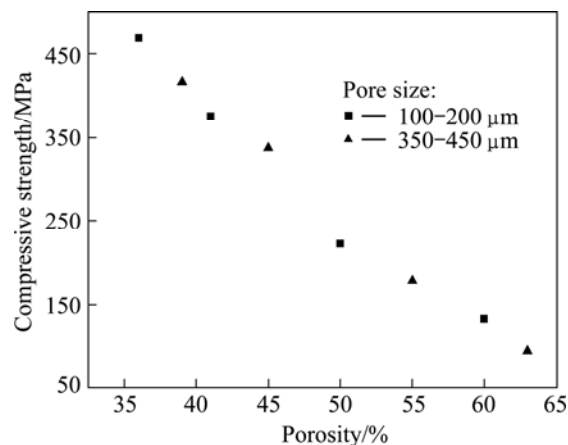


Fig. 4 Compressive strength of sintered porous titanium as function of porosity

The bulk implant materials which have higher stiffness than bone prevent the needed stress transferring to adjacent bone, resulting in bone resorption around the implant and consequently implant loosening. Thus, a material with an excellent combination of high strength and low modulus closer to the bone has to be used for implantation to avoid loosening of implants and higher service period to avoid revision surgery [13]. The human cancellous bone possesses an elastic modulus less than 3 GPa [14], while the stiffness of human compact bone ranges between 12 and 17 GPa [1]. Human bone's compression strength is in the range of 2–180 MPa [12]. In this work, the elastic modulus and compressive strength of porous Ti samples are found to be close to those of human bone. Therefore, this porous Ti can be considered promising biomedical materials.

3.2.3 Deformation mode of cell wall

Various empirical relations have been proposed to describe the dependence of mechanical properties of foams on their porosity content. GIBSON-ASHBY model assumed the pore walls as solid metal and found that the contribution of cell face stretching to the overall stiffness and strength of the foam is linearly dependent on the relative density term, ρ/ρ_s , while the contribution of cell edge bending is non-linear [12]. The density and yield stress of pure bulk Ti are 4.5 g/cm³ and 480 MPa, respectively. Figure 5 shows the compressive yield strength of the porous Ti (σ_{pl}) normalized to the yield strength of the solid metal (σ_s) as a function of relative density (ρ/ρ_s) and that predicted by the GIBSON-ASHBY model [12].

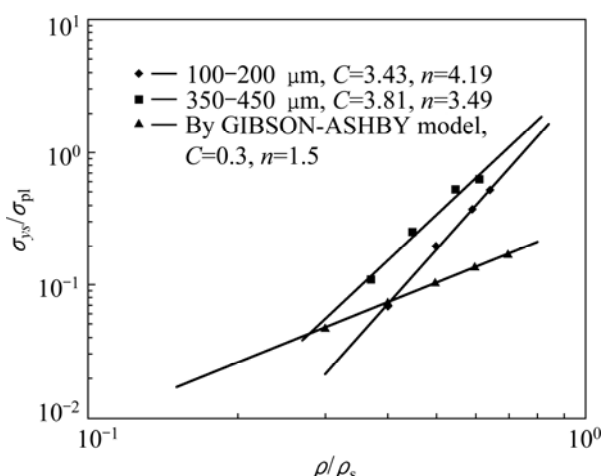


Fig. 5 Relative yield strength (σ_{pl}/σ_{ys}) of porous Ti as function of relative density (ρ/ρ_s) and prediction of GIBSON-ASHBY model for porous Ti

In GIBSON-ASHBY model, the strength of metallic foam is the collapse stress or plateau stress rather than the peak stress. Because the curves of specimens with higher relative densities do not have clear plateau regions, and the plateau stress is ambiguous, the plateau stress is substituted for the yield stress in Eq. (1). The axes are being scaled logarithmically, and the slope of the plots in Fig. 5 is the density exponent n in Eq. (1). From Fig. 5, the constant C and density exponent n for the two kinds of pore sizes are 3.43 and 3.81, 4.19 and 3.49, respectively. It is noted that there are a few differences in both of the constant C and density exponent n . According to Eq. (1), C is a constant for the geometric effect and the variation of C is probably due to heterogeneity in pore shape and size [15]. The shape of porous specimens is similar owing to the same kind of space particles. From Fig. 4, it is noted that pore size has no influence on the compressive strength of the porous Ti. But the value of constant C suggests that the pore sizes affected the yield strength of the porous Ti to some extent. It is reported that the value of n in Eq. (1) is governed by the deformation mode of the individual cell struts, i.e. yielding, bending, and buckling, and the value of n is in a wide range of 1.0–6.3 [16]. YAMADA et al [17] suggested the value of n for the cell wall or strut bending is 2 and that for struts buckling is 3, while the value of n is 1 for cell strut yielding. It is noted that the deformation mode can be divided into three regions by the critical value of n by 1, 2, and 3. In the present study, the experimental values of n are 3.49 and 4.19, both larger than the critical value of 3. Therefore, this suggests that the deformation mode of the porous Ti with a porosity ranging from 36% to 63% is mainly buckling of the cell struts.

4 Conclusions

1) Porous Ti with the porosities of 36%–63% for two different pore size distributions designed in advance, ranging from 100 to 200 μm and 350 to 450 μm , was fabricated by powder metallurgy using the space holder technique.

2) The elastic modulus and the compression strength decrease with the increase of porosities. It is worth noting that the relationship between the compressive strength and porosities is a completely linear relation beyond the effect of pore size distributions. The compression strength and the elastic modulus are in the range from 94.05 to 468.57 MPa and 2.662 to 18 GPa, respectively. The elastic modulus and compressive strength are found to be close to those of human bone. Thus, this porous Ti can be considered promising biomedical materials.

3) Constant C suggests that the pore sizes affect the yield strength of the porous Ti. The experimental values of n are 3.49 and 4.19, both larger than the critical value of 3, which indicates that the deformation mode of the porous Ti with a porosity ranging from 36% to 63% is mainly buckling of the cell struts.

References

- [1] LONG M, RACK H J. Titanium alloys in total joint replacement—A materials science perspective [J]. *Biomaterials*, 1998, 19: 1621–39.
- [2] OH I H, NOMURA N, MASAHASHI N, HANADA S. Mechanical properties of porous titanium compacts prepared by powder sintering [J]. *Scripta Materialia*, 2003, 49: 1197–202.
- [3] NOMURA N, KOHAMA T, OH I H, HANADA S, CHIBA A, KANEHIRA M, SASAKI K. Mechanical properties of porous Ti–15Mo–5Zr–3Al compacts prepared by powder sintering [J]. *Materials Science and Engineering C*, 2005, 25: 330–335.
- [4] KRISHNA B V, BOSE S, BANDYOPADHYAY A. Low stiffness porous Ti structures for load-bearing implants [J]. *Acta Biomaterialia*, 2007, 3: 997–1006.
- [5] KARAGEORGIOU V, KAPLAN D. Porosity of 3D biomaterial scaffolds and osteogenesis [J]. *Biomaterials*, 2005, 26: 5474–5491.
- [6] ITÄLÄ A I, YLÄNEN H O, EKHOLM C, KARLSSON K H, ARO H T. Pore diameter of more than 100 μm is not requisite for bone ingrowth in rabbits [J]. *Journal of Biomedical Materials Research*, 2001, 58: 679–683.
- [7] WEN C E, MABUCHI M, YAMADA Y, SHIMOJIMA K, CHINO Y, ASAHINA T. Processing of biocompatible porous Ti and Mg [J]. *Scripta Materialia*, 2001, 45: 1147–1153.
- [8] TAKEMOTO M, FUJIBAYASHI S, NEO M, SUZUKI J, KOKUBO T, NAKAMURA T. Mechanical properties and osteoconductivity of porous bioactive titanium [J]. *Biomaterials*, 2005, 26: 6014–6023.
- [9] PARTHASARATHY J, STARLY B, RAMAN S, CHRISTENSEN A. Mechanical evaluation of porous titanium (Ti6Al4V) structures with electron beam melting (EBM) [J]. *Journal of the Mechanical Behavior of Biomedical Materials*, 2010, 3: 249–259.
- [10] CHEN L J, LI T, LI Y M, HE H, HU Y H. Porous titanium implants fabricated by metal injection molding [J]. *Transactions of Nonferrous Metals Society of China*, 2009, 19: 1174–1179.

- [11] LIN Jian-guo, ZHANG Yun-fei, MA Mo. Preparation of porous Ti35Nb alloy and its mechanical properties under monotonic and cyclic loading [J]. Transactions of Nonferrous Metals Society of China, 2010, 20(3): 390–394.
- [12] GIBSON L J, ASHBY M F. Cellular solids: Structure and properties [M]. Cambridge: Cambridge Univ Pr, 1999.
- [13] GEETHA M, SINGH A K, ASOKAMANI R, GOGIA A K. Ti based biomaterials, the ultimate choice for orthopaedic implants—A review [J]. Progress in Materials Science, 2009, 54: 397–425.
- [14] TENCER F, JOHNSON K. Biomechanics in orthopaedic applications: Bone fracture and fixation [M]. London: Martin Dunitz, 1994.
- [15] WANG X, LI Y, XIONG J, HODGSON P D, WEN C E. Porous TiNbZr alloy scaffolds for biomedical applications [J]. Acta Biomaterialia, 2009, 5: 3616–3624.
- [16] HAKAMADA M, ASAO Y, KUROMURA T, CHEN Y, KUSUDA H, MABUCHI M. Density dependence of the compressive properties of porous copper over a wide density range [J]. Acta Materialia, 2007, 55: 2291–2299.
- [17] YAMADA Y, WEN C, SHIMOJIMA K, HOSOKAWA H, CHINO Y, MABUCHI M. Compressive deformation characteristics of open-cell Mg alloys with controlled cell structure [J]. Mater Trans, 2002, 43: 1298–1305.

不同孔径分布多孔钛的力学性能

王晓花, 李金山, 胡锐, 寇宏超, 周廉

西北工业大学 凝固技术国家重点实验室, 西安 710072

摘要: 从生物学角度出发设计并制备 2 种不同孔径分布的多孔钛, 并研究其力学性能。采用造孔剂烧结方法制备孔隙率为 36%~63%的多孔钛, 通过室温压缩测试其力学性能。多孔钛的弹性模量和抗压强度分别在 2.662~18 GPa 和 94.05~468.57 MPa 范围内, 且都随着孔隙率的增加而降低。抗压强度和孔隙率的关系曲线呈现完全的线性特征, 表明抗压强度主要受孔隙率的影响, 几乎不受孔径的影响。Gibson-Ashby 力学关系分析结果显示: 常数项 C 值的差异说明孔径分布对多孔钛的屈服强度有一定的影响; 密度指数 n 值均大于临界值 3, 表明这 2 种不同孔径的多孔钛的变形方式相同, 为孔壁的屈曲作用。

关键词: 多孔钛; 孔径分布; 力学性能; 密度指数; 生物材料

(Edited by Xiang-qun LI)